



EXTENDED ABSTRACT

**Microstructure, roughness, and corrosion resistance of X5CrNi18-10 austenite stainless steel welded joint\***

BOJANA M. RADOJKOVIĆ\*, BORE V. JEGDIĆ#, JOVANKA N. KOVAČINA#, SANJA I. STEVANOVIĆ# and DUNJA D. MARUNKIĆ#

*University of Belgrade, Institute of Chemistry, Technology and Metallurgy, Department of Electrochemistry, Njegoševa 12, Belgrade, Serbia*

(Received 3 December 2020, accepted 3 February 2021)

**Abstract:** The influence of the microstructure of X5CrNi18-10 stainless steel welded joint on its resistance to general, pitting, and intergranular corrosion was analyzed. The structure of weld metal, heat affected zone (HAZ) and base metal before and after electrochemical testing was analyzed using SEM/EDS. The influence of the roughness level of the welded joint on its resistance to the mentioned types of corrosion was also examined. Although the degree of sensitization of HAZ was significantly lower than the limit value, HAZ showed a noticeably greater tendency to general and pitting corrosion than weld metal and base metal. Polishing has been shown to improve significantly the corrosion resistance of HAZ than in other parts of a welded joint.

**Keywords:** test methods; electrochemistry; SEM/EDS; AFM.

INTRODUCTION

Welded joints of X5CrNi18-10 stainless steel, under certain conditions, have a tendency towards various types of localized corrosion, such as pitting corrosion, intergranular corrosion, stress corrosion cracking, etc. This poses a major problem in the application of these steels in various industries.

Localized corrosion of stainless steel occurs especially in the presence of chloride ions.<sup>1</sup> Intergranular corrosion occurs along chromium-depleted zones that are formed, for example, in the heat affected zone (HAZ) during welding.<sup>2</sup> The places where pitting corrosion occurs are MnS inclusions, chromium-depleted zones in the HAZ, as well as austenite/ferrite boundaries in the weld metal.<sup>3–7</sup>

\* Corresponding author. E-mail: bojana.radojkovic@ihtm.bg.ac.rs

• The lecture held at the meeting of the Electrochemical Division of the Serbian Chemical Society in Belgrade on October 26th, 2020.

# Serbian Chemical Society member.

<https://doi.org/10.2298/JSC201203007R>

There is great disagreement regarding the influence of surface roughness levels on corrosion resistance of stainless steels and other alloys.<sup>8–10</sup> While some deny this effect, others show that there is a direct effect of roughness on corrosion resistance.

In this abstract, the influence of the microstructure of welded joint and surface roughness on resistance to general and pitting corrosion, as well as on the stability of passive film was investigated.

#### EXPERIMENTAL

Welding of the X5CrNi18-10 stainless steel was performed by the TIG process using constant welding parameters (welding rate 5 cm min<sup>-1</sup>, current level 150 A, heat input 14.6 kJ cm<sup>-1</sup>), using argon as shielding gas. The microstructure of individual parts of the welded joint before and after electrochemical testing was analyzed using an SEM/EDS microscope. Having in mind the small dimensions of the welded joint zones, a small electrochemical cell was constructed that enables such tests.

In order to determine the resistance to general and pitting corrosion, polarization measurements were performed in an NaCl solution. Testing of intergranular corrosion was performed by the electrochemical potentiokinetic reactivation method with a double loop (DL EPR). Electrochemical tests were also performed on welded joint specimens with different roughness. The morphology and degree of roughness were analyzed using atomic force microscopy (AFM).

#### RESULTS AND DISCUSSION

The characteristic parts of a welded joint are shown in Fig. 1. These parts differ in microstructure and show different corrosion resistance.

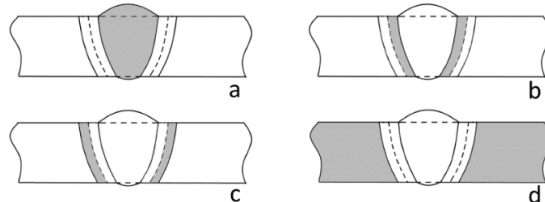


Fig. 1. Parts of the welded joint: a) weld metal, b) HAZ with coarse grain, c) HAZ and d) base metal.

In the weld metal (Fig. 1a) during solidification, a dendritic austenite/ferrite microstructure is formed.<sup>2</sup> Directly to the weld metal, a narrow zone is formed in which, due to the large heat input during welding, a significant grain growth occurred (Fig. 1b). The grain size in this zone ranged from 46 to 69 µm.

In the HAZ (Fig. 1c) during welding, chromium carbides are precipitated at the grain boundary, resulting in the formation of the chromium-depleted zones.<sup>2</sup> Particularly sensitive to pit formation are the places where MnS inclusions intersect these zones. In the HAZ, the grain size was the same as for the base metal (from 18 to 20 µm). In the base metal, there are no microstructural changes.

AFM 3D plots of grinded and polished specimens are shown Fig. 2. Unlike the ground specimen, no grooves were seen on the polished specimen. The RMS value in the ground specimen was 54.0 nm, while in the polished one it was 3.6 nm.

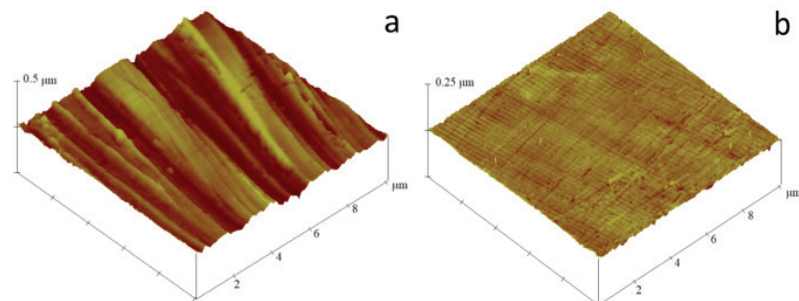


Fig. 2. AFM plots in a 3D perspective: a) ground and b) polished surface of stainless steel.

The intergranular corrosion was tested using the DL EPR method. The ratio of the reactivation current  $I_r$  and the passivation current  $I_p$ , taking into account the grain size G ( $G \approx 9$ ), is a measure of the resistance of stainless steel to intergranular corrosion:

$$\left( \frac{I_r}{I_p} \right)_{GBA} = \frac{I_r}{I_p \left( 10^{-3} \sqrt{2^{G+5}} \right)} \quad (1)$$

The ratio  $(I_r/I_p)_{GBA}$  for HAZ was about 3.5 times below the limit value defined by the ISO standard, while in the base metal, this ratio was even lower (Fig. 3). The relatively low value of  $(I_r/I_p)_{GBA}$  is a consequence of the low carbon content in the stainless steel.

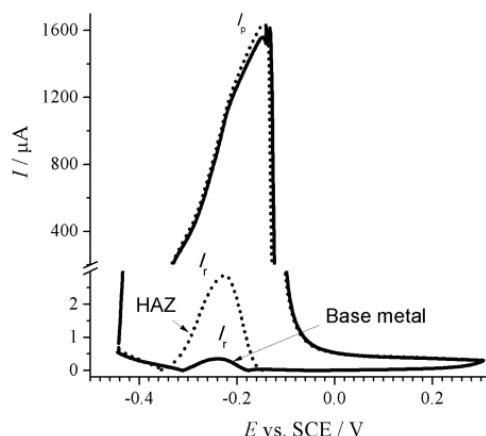


Fig. 3. DL EPR diagram.

The results presented in Fig. 4 show that the HAZ resistance to general corrosion is reduced and the susceptibility to pitting corrosion (compared to the base metal) is increased. This could only be a consequence of the formation of chromium-depleted zones along the grain boundaries in the HAZ.

At potentials lower than  $E_{\text{pit}}$  (Fig. 4), current peaks are visible, which indicate the formation of metastable pits. At potentials above  $E_{\text{pit}}$ , the pits grow steadily. The weld metal had the highest resistance to general and pitting corrosion due to its higher content of chromium and nickel than in the base metal. The results of electrochemical tests are summarized in Table I.

TABLE I. Results of electrochemical testing of ground and polished welded joint

Sample		$I_{\text{corr}} / \text{nA}$	$I_{\text{pass}} / \text{nA}$	$E_{\text{mpit}} / \text{mV}$	$E_{\text{pit}} / \text{mV}$
Base metal	Grinded	5.5	28	336	387
	Polished	1.5	2.0	387	387
Weld metal	Grinded	6.0	25	326	430
	Polished	1.4	2.2	427	427
HAZ	Grinded	14	40	278	346
	Polished	2.4	3.3	378	378

The polarization curves obtained for polished specimens (Fig. 5) do not contain the characteristic passivation peak, which is visible in the polarization curves in Fig. 4. Besides, metastable pits are not formed. A single pit is probably formed, which continues to grow.

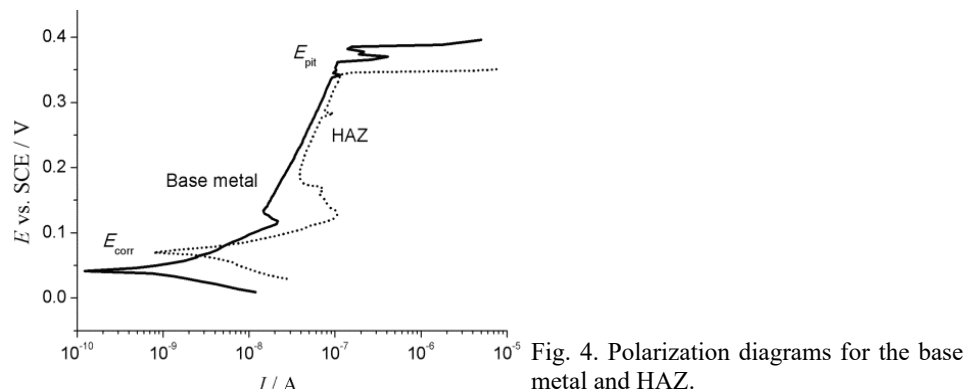


Fig. 4. Polarization diagrams for the base metal and HAZ.

The roughness noticeably affects a change in the corrosion resistance in HAZ. The  $E_{\text{pit}}$  value for the ground surface was  $\approx 350$  mV while for the polished HAZ surface it was  $\approx 380$  mV. This is very important because HAZ has a critical place for a welded joint for various types of corrosion. In addition, the polished specimen shows higher resistance to general corrosion, and a more stable passive film (Fig. 5). The real surface of the ground specimen is larger than that of the polished one. A passive film is less stable at the peaks of the grinded surface.

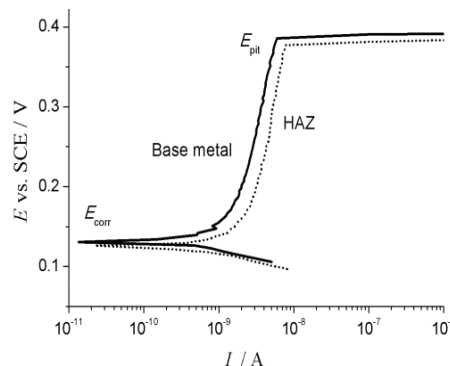


Fig. 5. Polarization diagrams for polished surfaces of the base metal and HAZ.

During pit formation (Fig. 6), first Mn and S dissolve from the inclusions and their dimensions are reduced. At the boundary of the inclusion with the matrix, a channel is created where metastable pits are formed first, as well as stable pits that continue to grow.<sup>3</sup> That the pit was formed in trenches around the central part of the inclusion is shown in Fig. 6b.

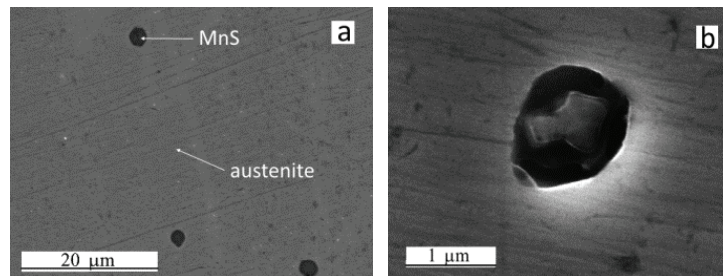


Fig. 6. SEM microphotographs of pit formation stages at MnS inclusions in HAZ.

In the weld metal, pits are most often formed at the austenitic/ferrite boundary (Fig. 7). EDS analysis showed that the chromium content in  $\delta$ -ferrite is higher than in the austenitic matrix. However, several pits were also formed at a certain distance from  $\delta$ -ferrite in the austenitic matrix.

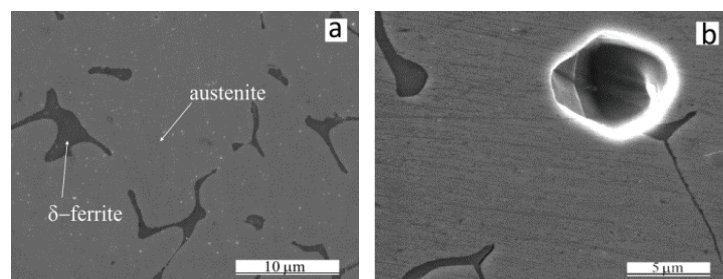


Fig. 7. SEM microphotographs of weld metal: a) before and b) after polarization measurements.

## CONCLUSIONS

This paper analyzes the influence of microstructure and roughness levels of the welded joint of X5CrNi18-10 stainless steel on its resistance to general, pitting, and intergranular corrosion.

The polished specimen had greater resistance to general corrosion than the grinded specimen, in all three parts of the welded joint (weld metal, HAZ and base metal). This difference is especially noticeable in the HAZ. Moreover, a passive film on the polished surface is more stably related to the ground surface. In HAZ, the values of the pitting potential  $E_{\text{pit}}$  and the potential of metastable pitting  $E_{\text{mpit}}$  for the polished surface are significantly higher than are those for the ground surface. This is very important because HAZ is a critical place for a welded joint for various types of corrosion.

*Acknowledgment.* This work was financially supported by the Ministry of Education, Science and Technological Development of the Republic of Serbia (Grant No. 451-03-68/2020-14/200026).

### И З В О Д

### Х МИКРОСТРУКТУРА, ХРАПАВОСТ И ОТПОРНОСТ НА КОРОЗИЈУ ЗАВАРЕНОГ СПОЈА АУСТЕНИТНОГ НЕРЂАЈУЋЕГ ЧЕЛИКА X5CrNi18-10

БОЈАНА М. РАДОЈКОВИЋ, БОРЕ В. ЈЕГДИЋ, ЈОВАНКА Н. КОВАЧИНА, САЊА И. СТЕВАНОВИЋ  
и ДУЊА Д. МАРУНКИЋ

*Универзитет у Београду, Институт за хемију, технологију и металургију, Центар за електрохемију,  
Његошева 12, 11000 Београд*

Анализиран је утицај микроструктуре завареног споја нерђајућег челика X5CrNi18-10 на његову отпорност према општој, питинг и интеркристалној корозији. Структура метала шава, зоне утицаја топлоте (HAZ) и основног метала, пре и после електрохемијских испитивања, анализирана је применом SEM/EDS. Такође испитан је утицај нивоа храпавости завареног споја на његову отпорност према наведеним видовима корозије. Иако је степен сензибилизације HAZ био знатно нижи од граничне вредности, ЗУТ је показао значајно већу склоност према општој и питинг корозији него метал шава и основни метал. Показано је да полирање знатно побољшава отпорност ЗУТ према корозији него што је то случај са осталим деловима завареног споја.

(Примљено 3. децембра 2020, прихваћено 3. фебруара 2021)

### REFERENCES

1. H. Bohni, *Localized Corrosion of Passive Metals*, in *Uhlig's Corrosion Handbook*, R. W. Revie, Ed., John Wiley & Sons, Inc, Hoboken, NJ, 2011, p. 157 (<https://doi.org/10.1002/9780470872864>)
2. J. R. Davis, *Corrosion of Weldments*, ASM International, Materials Park, OH, 2006, p. 43 (<https://doi.org/10.1361/corw2006p001>)
3. A. Chiba, I. Muto, Y. Sugawara, N. Hara, *J. Electrochem. Soc.* **160** (2013) C511 (<https://doi.org/10.1149/2.081310jes>)
4. N. Ida, I. Muto, Y. Sugawara, N. Hara, *J. Electrochem. Soc.* **164** (2017) C779 (<https://doi.org/10.1149/2.1011713jes>)

5. B. T. Lu, Z. K. Chen, J. L. Luo, B. M. Patchett, Z. H. Xu, *Electrochim. Acta* **50** (2005) 1391 (<http://dx.doi.org/10.1016/j.electacta.2004.08.036>)
6. B. Jegdić, B. Bobić, B. Radojković, B. Alić, Lj. Radovanović, *J. Mater. Process. Technol.* **266** (2019) 579 (<https://doi.org/10.1016/j.jmatprotec.2018.11.029>)
7. B. Radojković, J. Kovačina, B. Jegdić, B. Bobić, B. Alić, D. Marunkić, A. Simović, *Mater. Corros.* (2020) 1, accepted (<https://doi.org/10.1002/maco.202012039>)
8. H. Ezuber, A. Alshater, S. O. Nisar, A. Gonsalvez, S. Aslam, *Surf. Eng. Appl. Electrochem.* **54** (2018) 73 (<https://doi.org/10.3103/S1068375518010039>)
9. M. J. Seo, H.-S. Shim, K. M. Kim, S.-I. Hong, D. H. Hur, *Nucl. Eng. Des.* **280** (2014) 62 (<http://dx.doi.org/10.1016/j.nucengdes.2014.08.023>)
10. S. Reinemann, P. Rosemann, M. Babutzka, J. Lehmann, A. Burkert, *Mater. Corros.* **70** (2019) 1776 (<https://doi.org/10.1002/maco.201910874>).